THE JOURNAL OF PHYSICAL CHEMISTRY A LETTERS

2005, *109,* 3527−3530
Published on Web 03/30/2005

Dynamics of the O(^{3}P) + C$_2$H$_4$ Reaction: Identification of Five Primary Product Channels (Vinoxy, Acetyl, Methyl, Methylene, and Ketene) and Branching Ratios by the Crossed Molecular Beam Technique with Soft Electron Ionization

Piergiorgio Casavecchia,* Giovanni Capozza, Enrico Segoloni, Francesca Leonori, Nadia Balucani, and Gian Gualberto Volpi

Dipartimento di Chimica, Università di Perugia, 06123 Perugia, Italy

Received: February 4, 2005; In Final Form: March 9, 2005

The crossed molecular beam scattering technique with soft electron ionization (EI) is used to disentangle the complex dynamics of the polyatomic O(^{3}P) + C$_2$H$_4$ reaction, which is of great relevance in combustion and atmospheric chemistry. Exploiting the newly developed capability of attaining universal product detection by using soft EI, at a collision energy of 54.0 kJ mol^{-1}, five different primary products have been identified, which correspond to the five exoergic competing channels leading to CH$_2$CHO(vinoxy) + H, CH$_3$CO(acetyl) + H, CH$_3$(methyl) + HCO(formyl), CH$_2$(methylene) + HCHO(formaldehyde), and CH$_2$CO(ketene) + H$_2$. From laboratory product angular and velocity distributions, center-of-mass product angular and translational energy distributions and the relative branching ratios for each channel have been obtained, affording an unprecedented characterization of this important reaction.

I. Introduction

Gas-phase chemical reactions relevant in areas of practical interest—from combustion science to terrestrial/planetary atmospheres and interstellar clouds—commonly encompass polyatomic molecules/radicals and usually involve several product channels. Three basic goals are to determine (a) the nature of the primary products, (b) the dynamics of their formation, and (c) their relative yield (branching ratios). The most suitable technique to tackle this challenge is the crossed molecular beam (CMB) scattering technique with velocity analysis, based on electron−ionization (EI) mass-spectrometric (MS) detection.[1−3] In fact, EI is a universal detection method because every species can be ionized at the electron energies (60−200 eV) normally used in MS instruments. For this reason, the EI-MS technique has been extensively used in CMB investigations;[1−3] unfortunately, when applied to studies of polyatomic reactions, the method is plagued by the problem of the dissociative ionization of reactants, products, and background gases.[3] To reduce this problem, the technique of soft ionization by tunable low-energy electrons has recently been implemented in CMB experiments,[4,5] following the example of the soft photoionization (PI) technique via VUV tunable radiation from third-generation synchrotrons.[6−10] The use of soft EI is much simpler than that of soft PI and offers the possibility of determining branching ratios because absolute EI cross sections are often known or reliably estimated.[3,9−11] Soft EI was not applied in CMB experiments in the past for reasons associated with the signal-to-noise ratio because EI cross sections drop drastically with decreasing electron energy. Very recently, however, we have successfully demonstrated its feasibility in CMB studies of the O(^{3}P) + C$_2$H$_2$ reaction, where the two competing pathways leading to HCCO + H and CH$_2$ + CO formation were readily characterized.[4]

In this letter, we report on a detailed CMB investigation of the reaction between ground-state oxygen atoms O(^{3}P) and ethylene, which is of great relevance in combustion and atmospheric chemistry.[12,13] The reaction of O(^{3}P) with ethylene is significantly more complex than that with acetylene. The following five exoergic reactions have been considered as possible primary channels:

$$\mathrm{O(^3P) + C_2H_4 \rightarrow H + CH_2CHO} \quad \Delta H^\circ = -71\ \mathrm{kJ\ mol^{-1}} \tag{1a}$$

$$\rightarrow \mathrm{H + CH_3CO} \quad \Delta H^\circ = -114\ \mathrm{kJ\ mol^{-1}} \tag{1b}$$

$$\rightarrow \mathrm{H_2 + CH_2CO} \quad \Delta H^\circ = -356\ \mathrm{kJ\ mol^{-1}} \tag{1c}$$

$$\rightarrow \mathrm{CH_3 + HCO} \quad \Delta H^\circ = -113\ \mathrm{kJ\ mol^{-1}} \tag{1d}$$

$$\rightarrow \mathrm{CH_2 + HCHO} \quad \Delta H^\circ = -29\ \mathrm{kJ\ mol^{-1}} \tag{1e}$$

Over the last 50 years, many research groups have investigated the kinetics of reaction 1 by employing a variety of experimental techniques under different conditions.[13−24] Although its overall rate constant has been well established,[20,21] the identity of the primary products and their relative branching ratios has been the subject of considerable controversy[21,22] (Table 1). However, knowledge of these entities is of primary importance for modeling combustion systems as well as atmospheric and outer-space chemistry. Very recently, the rovibrational energy distribution of the HCO product has been

---

* Corresponding author. E-mail: piero@dyn.unipg.it.

10.1021/jp050627+ CCC: $30.25

TABLE 1: History of the Branching Ratios, $\sigma_i/\sum\sigma_i$, for the $O(^3P) + C_2H_4$ Reaction

	product				
reference	CH_2CHO	CH_3CO	CH_2CO	CH_3	CH_2
Cvetanovic[13]	<0.10		0.04		
Gutman[14]	≪0.10		large	large	
Hunzinger[15]	0.36 ± 0.04			0.52−0.58	
Kaufman[17]	0.79 ± 0.14				
Klemm[18]	0.27 ± 0.05				
Endo[19]	0.4 ± 0.1			0.5 ± 0.1	0.1 ± 0.05
Temps[21]	0.50 ± 0.10		0	0.44 ± 0.15	0.06 ± 0.03
Schmoltner[22]	0.29 ± 0.11			0.71 ± 0.26	-
this work	0.27 ± 0.06	0.01 ± 0.005	0.13 ± 0.03	0.43 ± 0.09	0.16+0/−0.08

determined by laser-induced fluorescence in a flow system,[23] and the infrared chemiluminescence of some primary and secondary products has also been measured in flow at room temperature.[24] The $O(^3P) + C_2H_4$ reaction has also been tackled by the CMB technique. In the early 1980s, two different CMB studies[16] at a collision energy of $E_c \approx 25$ kJ mol^{-1} were able to characterize only channel 1a. Channel 1b leading to CH_3CO (an isomer of CH_2CHO) could not be disentangled. Channels 1c−1e could not be detected because, besides the unfavorable kinematics, the expected ion signal from their products coincides with major background peaks and/or with peaks coming from the dissociative ionization of the most intense CH_2CHO product and of the elastically scattered C_2H_4 reagent. Only the problem connected with channel 1d was partially overcome in a later CMB study[22] by using isotopically labeled ^{18}O, which permitted the detection of the $HC^{18}O$ product at $m/z = 31$ and 30 ($C^{18}O^+$), and then an estimate of the branching ratio of cross sections, σ, was obtained. The derived value of $\sigma_{1d}/(\sigma_{1d} + \sigma_{1a}) = 0.71 \pm 0.26$ is somewhat larger than previous kinetic estimates (at 300 K), which range from 0.44 to 0.55 (Table 1).[25]

In the present work, by coupling an improved CMB instrument with a tunable ionizer (7−100 eV) and exploiting soft EI, we have been able to avoid most of the above complications. From detailed measurements of angular and velocity distributions at selected *m/z* values, it has been possible to identify as primary products the vinoxy, acetyl, methyl, and methylene radicals and the ketene molecule and hence to characterize the reaction dynamics of all five competing channels (1a−1e) and determine their branching ratios.

II. Experimental Method and Results

Product angular, $N(\Theta)$, and TOF, $N(\Theta, t)$, distributions were measured at different energies of the ionizing electrons using supersonic beams of $O(^3P)$ and C_2H_4 with peak velocities of 2739 and 808 m s^{-1}, respectively. A new configuration of the CMB apparatus, with an intersection angle of the two beams of 135°, allowed us higher TOF resolution, which was essential to disentangle the different contributions to each *m/z* signal. The resulting E_c was 54.0 kJ mol^{-1}. The basics of the CMB apparatus and atomic oxygen beam source have been described elsewhere.[26] The $N(\Theta)$ at $m/z = 15$ measured with 17 eV electron energy (the value required to suppress the interfering contributions at $m/z = 15$, as CH_3^+ and $^{13}CH_2^+$, from elastically scattered C_2H_4 because the appearance energy AE of these ions from C_2H_4 is 17 and 18 eV, respectively) is shown in Figure 1 together with the velocity vector (Newton) diagram of the experiment. At 17 eV, the $m/z = 15$ signal, besides that from the CH_3 product of channel (1d), partially originates from CH_2CHO/CH_3CO via dissociative ionization, but the various contributions to the $m/z = 15$ signal can be easily separated by performing velocity distribution measurements at selected laboratory angles by the TOF method. (See below.) Figure 2 shows exemplary TOF spectra recorded at $m/z = 42$, 15, and 14 for the laboratory angle $\Theta = 34°$. It should be noted that the vinoxy product could not be detected via the highly unstable parent CH_2CHO^+ ion ($m/z = 43$) but only via the daughter ion ($m/z = 42$) (Figure 3). As derived from the data analysis[26] and clearly shown in Figure 2, the TOF spectra carry the fingerprints of all five reaction channels. Specifically, the $m/z = 42$ TOF spectrum exhibits (i) a dominant peak due to the fragmentation of CH_2CHO^+ (channel 1a), (ii) a faster peak, appearing as a shoulder on the main peak, which is unambiguously attributed, on the basis of the total energy and linear momentum conservation, to the ketene product from channel 1c, and (iii) a small, slow component, which peaks at the CM velocity and has been attributed to the fragmentation of CH_3CO^+ from channel 1b with low recoil energy. The $m/z = 15$ TOF spectrum exhibits a fast peak that is unambiguously attributed to CH_3 from channel 1d and a slower, more intense peak analogous to the main peak observed at $m/z = 42$, which is due to dissociative ionization of the vinoxy product (channel 1a). Note that the small contribution of CH_3CO is not visible in the TOF spectrum at $m/z = 15$, presumably because of the different fragmentation patterns of the internally hot vinoxy and acetyl radicals. The two reactive channels are characterized, in fact, by a different exoergicity, and their dynamics appear to differ dramatically.

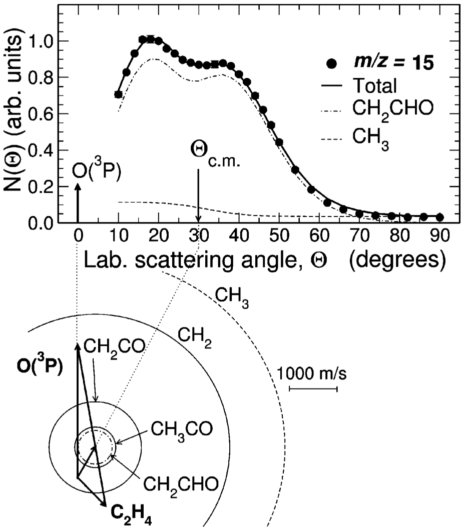

Figure 1. Laboratory angular distribution at $m/z = 15$ (●) from the reaction of $O(^3P) + C_2H_4$ at $E_c = 54.0$ kJ mol^{-1}, obtained by using an electron energy of 17 eV, together with the relative Newton diagram. Error bars are smaller than the experimental dots. The circles in the Netwon diagram delimit the maximum speed that the indicated products can attain on the basis of energy and linear momentum conservation if all of the available energy goes into product translation. The heavy solid line is the total angular distribution calculated from the best-fit product CM translational energy and angular distributions, the separate contributions from the CH_2CHO and CH_3 products from channels 1a and 1d being shown with light continuous and dotted lines, respectively.

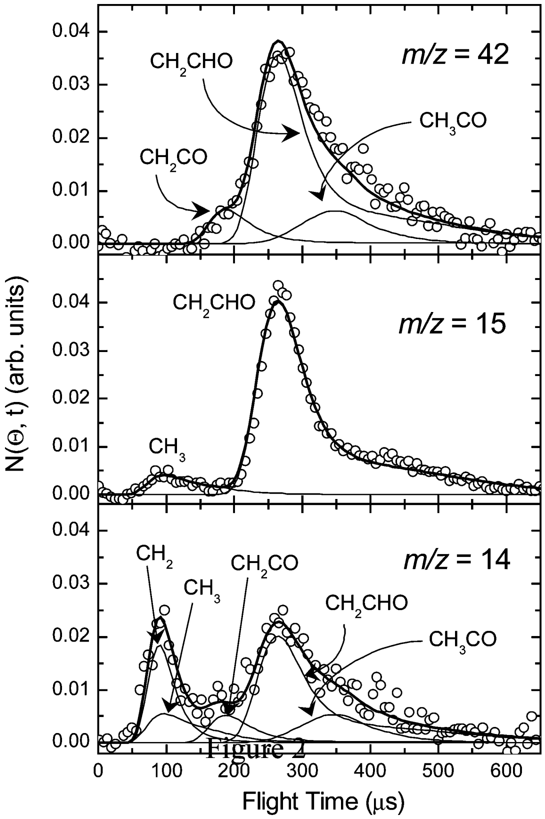

Figure 2. TOF spectra at $\Theta = 34°$ for the $O(^3P) + C_2H_4$ reaction at $E_c = 54.0$ kJ mol^{-1} recorded at $m/z = 42$, 15, and 14 using an electron energy of 17 eV. Open circles are experimental points; heavy solid lines are the total TOF distributions calculated from the best-fit product CM translational energy and angular distributions for the contributing channels. The various contributions (depicted with light solid lines) are marked with the formula of the corresponding product. Relative intensities at the TOF highest peak for $m/z = 42$, 15, and 14 are 1.0, 3.0, and 0.23, respectively.

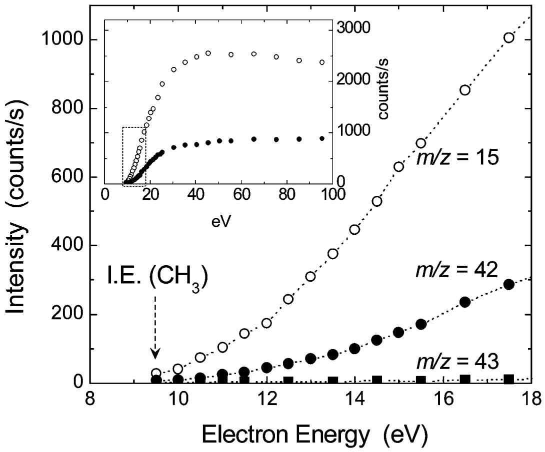

Figure 3. Electron ionization efficiency curves as a function of electron energy for the indicated m/z values recorded at $\Theta = 34°$. (The lines through the experimental points are to guide the eye.) Note that there is no parent CH_2CHO^+, the very small intensity at $m/z = 43$ being due to $^{13}C_2H_2O^+$. The inset shows the efficiency curves for $m/z = 15$ and 42 from the threshold up to 100 eV. Relative count rates are at the CM angle using an electron emission current of 1 mA.

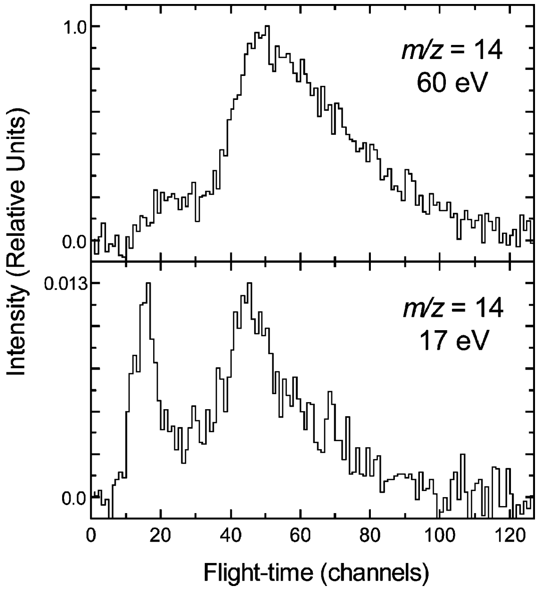

Figure 4. TOF spectra for the $O(^3P) + C_2H_4$ reaction at (top) $m/z = 14$ and 60 eV electron energy, reflecting C_2H_4 (detected at $m/z = 14$ as CH_2^+) elastically scattered from O (slow peak) and undissociated O_2 (fast shoulder) contained in the oxygen beam and (bottom) $m/z = 14$ and 17 eV electron energy, reflecting only reactive scattering signals because the elastic contribution has been completely suppressed. (See text.) Note the relative scale of the two spectra: the reactive signal at $m/z = 14$ (17 eV) is on the order of 1% of the elastic signal at $m/z = 14$ (60 eV).

The $m/z = 14$ TOF spectrum appears to be more complex with a fast peak that can correspond only, on the basis of energy and linear momentum conservation, to CH_2 (methylene) formation from channel 1e, and several other contributions clearly originating from the fragmentation of vinoxy, acetyl, and ketene products (channels 1a−1c). A small contribution to the fast peak arises from the fragmentation of CH_3 from channel 1d. (The appearance energy, AE, of CH_2^+ from CH_3 is in fact 15.1 eV.[27]) We emphasize here that the use of soft EI is particularly crucial for the detection of CH_2 from channel 1e. In fact, because the AE of CH_2^+ from C_2H_4 is 18.0 eV,[27] by using an electron energy of 17 eV it was possible to remove completely the elastic contribution due to C_2H_4, which otherwise would overwhelm (by a factor ~100) the reactive signal (Figure 4). At the same time, at 17 eV the background at $m/z = 14$ due to dissociative ionization of residual N_2 becomes zero because the AE of N^+ from N_2 is 24.3 eV.[27] Using 17 eV, only some (unavoidable) dissociative ionization from the CH_2CHO, CH_3CO, and CH_2CO products remains, which, however, can be easily disentangled by TOF measurements at different m/z values (Figure 2).

Once the origin of the various ion signals is sorted out, the relative yield of each product can be derived from the estimated ionization cross section and the measured total ion yield for a specific product.[3,22] The branching ratios derived in this study are compared with previous kinetic and CMB estimates in Table 1. We note that CMB and kinetics experiments are relative to different E_c values; however, the branching ratios are not expected to exhibit a pronounced energy dependence in the $O + C_2H_4$ system because even at thermal energies the total available energy is well above the height of the interconversion and exit barriers in the potential energy surface (PES). (See schematic energy diagrams in refs 23, 24, and 28.) Under our experimental conditions, methyl + formyl formation is the dominant channel accounting for 43% of the yield, followed by vinoxy + H (27%). This is in line with most kinetic findings at 300 K. In addition, we have established that methylene + formaldehyde is formed in a significant fraction, thus corroborating the conclusions of recent kinetic investigations,[19,21] and we have disentangled and estimated the contributions of channels 1b and 1c. In particular, the formation of molecular products $CH_2CO + H_2$ has a sizable yield (more than 10%). It should be noted that the occurrence of channels 1b and 1c was also qualitatively invoked in the previous CMB study by Schmoltner et al.[22] to explain some features of the TOF spectra, which looked qualitatively similar to those observed in the present study. However, because of the lower S/N ratio, limited data set, and ion fragmentation problems, no definite and quantitative conclusions could be drawn in the earlier work.[22]

Notably, our results indicate that intersystem crossing (ISC) plays an important role in the title reaction because the occurrence of channels 1b−1d, which account for more than 50% of the reaction yield, can be rationalized only by assuming that ISC between triplet and singlet PESs takes place.[28] In fact, the variety of observed products arises from competition between (a) H elimination and C−C bond breaking (leading to $CH_2CHO + H$ and $CH_2 + HCHO$ formation, respectively) from the diradical adduct on the triplet PES and (b) ISC from the triplet to the singlet PES followed by H and H_2 elimination and C−C bond cleavage. (See PES in refs 22 and 28). A complete report on our results relative to all channels, including the derivation of center-of-mass product angular and translational-energy distributions, will be given in a future full publication. More measurements at different collision energies are under way.

III. Conclusions

We have demonstrated that by exploiting soft EI in CMB experiments it has become possible to characterize the dynamics of complex multichannel reactions, such as $O + C_2H_4$, by identifying all possible competing product channels (i.e., the so-called universal product detection has been attained) and determining their branching ratios. Besides affording a deeper understanding of complex chemical reactions, such as the important title reaction, the present work has far-reaching significance because similar studies, thanks to the use of soft EI, can be readily extended to a large variety of polyatomic reactions of wide practical interest, from combustion to atmospheric and astrochemistry, such as, for instance, those also involving C and N atoms with hydrocarbons, and possibly also to radical−radical polyatomic reactions.

Acknowledgment. This work was supported by the Italian MIUR (Ministero Istruzione, Università, Ricerca) via COFIN 2003 and FIRB 2001.

References and Notes

(1) Lee, Y. T.; McDonald, J. D.; Le Breton, P. R.; Herschbach, D. R. *Rev. Sci. Instrum.* **1969**, *40*, 1402−1408.

(2) Casavecchia, P. *Rep. Prog. Phys.* **2000**, *63*, 355−414, and references therein.

(3) Lee, Y. T. in *Atomic and Molecular Beam Methods, Vol. 1*, (ed. Scoles, G.), Oxford University Press: New York, 1987; pp 553−568.

(4) Capozza, G.; Segoloni, E.; Leonori, F.; Volpi, G. G.; Casavecchia, P. *J. Chem. Phys.* **2004**, *120*, 4557−4560.

(5) Casavecchia, P.; Capozza, G.; Segoloni, E. In *Modern Trends in Chemical Reaction Dynamics, Experiment and Theory (Part II)*; Yang, X.; Liu, K., Eds.; (*Adv. Series in Phys. Chem.* Vol. 14); World Scientific: Singapore, 2004; Ch. 7.

(6) Yang, X.; Lin, J.; Lee, Y. T.; Blank, D. A.; Suits, A. G.; Wodtke, A. M. *Rev. Sci. Instrum.* **1997**, *68*, 3317−3326.

(7) Wang, C. C.; Lee, Y. T.; Lin, J. J.; Yang, X. *J. Chem. Phys.* **2002**, *117*, 153−160.

(8) Blank, D. A.; Hemmi, N.; Suits, A. G.; Lee, Y. T. *Chem. Phys.* **1998**, *231*, 261−278; Hemmi, N.; Suits, A. G. *J. Chem. Phys.* **1998**, *109*, 5338−5343.

(9) Blank, D. A.; Sun, W. Z.; Suits, A. G.; Lee, Y. T.; North, S. W.; Hall, G. E. *J. Chem. Phys.* **1998**, *108*, 5414−5425; Robinson, J. C.; Harris, S. A.; Sun, W. Z.; Sveum, N. E.; Neumark, D. M. *J. Am. Chem. Soc.* **2002**, *124*, 10211−10224, and references therein.

(10) Recently, single photon PI by a 157 nm F_2 laser (7.9 eV radiation) has been successfully used in CMB studies of transition metal reactions exploiting the low ionization potentials of these metals and their compounds. See Hinrichs, R. Z.; Schroeden, J. J.; Davis, H. F. *J. Am. Chem. Soc.* **2003**, *125*, 860−861, and references therein.

(11) Fitch, W. L.; Sauter, A. D. *Anal. Chem.* **1983**, *55*, 832−835.

(12) Gardiner, W. C., Jr. *Gas-Phase Combustion Chemistry*, Springer-Verlach, New York, 2000.

(13) Cvetanović, R. J. *J. Chem. Phys.* **1955**, *23*, 1375−1380; Cvetanović, R. J.; Singleton, D. L. *Reviews Chem. Int.* **1984**, *5*, 183−226.

(14) Kanofsky, J. R.; Gutman, D. *Chem. Phys. Lett.* **1972**, *15*, 236−239.

(15) Hunzinger, H. E.; Kneppe, H.; Wendt, H. R. *J. Photochem.* **1981**, *17*, 377−387.

(16) Buss, R. J.; Baseman, R. J.; He, G.; Lee, Y. T. *J. Photochem.* **1981**, *17*, 389−396; Clemo, A. R.; Duncan, G. L.; Grice, R. *J. Chem. Soc., Faraday Trans.* 2 **1982**, *78*, 1231−1238.

(17) Sridharan, U. C.; Kaufman, F. *Chem. Phys. Lett.* **1983**, *102*, 45−49.

(18) Smalley, J. F.; Nesbitt, F. L.; Klemm, R. B. *J. Phys. Chem.* **1986**, *90*, 491−497.

(19) Endo, Y.; Tsuchiya, S.; Yamada, C.; Hirota, E.; Koda, S. *J. Chem. Phys.* **1986**, *85*, 4446−4452.

(20) Mahmud, K.; Marshall, P.; Fontijn, A. *J. Phys. Chem.* **1987**, *91*, 1568−1573.

(21) Bley, U.; Dransfeld, P.; Himme, B.; Koch, M.; Temps, F., Wagner, H. G. *22nd Symposium (International) on Combustion* (The Combustion Institute, Pittsburgh, 1988), p 997−1006.

(22) Schmoltner, A. M.; Chu, P. M.; Brudzynski, R. J.; Lee, Y. T. *J. Chem. Phys.* **1989**, *91*, 6926−6936.

(23) Gardner, J. L.; Miller, S. M. *J. Chem. Phys.* **2004**, *121*, 5920−5928.

(24) Dodd, J. A.; Hwang, E. S.; Castle, K. J.; DeBoer, G. D. *J. Phys. Chem. A*, **2004**, *108*, 10965−10972.

(25) The branching ratios derived in ref 22 were later revised by Morton, M. L.; Szpunar, D. E.; Butler, L. J. *J. Chem. Phys.* **2001**, *115*, 204−216.

(26) Alagia, M.; Balucani, N.; Casavecchia, P.; Stranges, D.; Volpi, G. G. *J. Chem. Soc., Faraday Trans.* **1995**, *91*, 575−596.

(27) NIST Chemistry WebBook, 2002.

(28) Fueno, T.; Takahara, Y.; Yamaguchi, K. *Chem. Phys. Lett.* **1990**, *167*, 291−297.